Molecular dynamics simulation study of structural, elastic and thermodynamic properties of tin below 286 K

A. Berroukche[1], B. Soudini[1,*], K. Amara[2]

[1] *Applied Materials Laboratory, University of Sidi Bel-Abbès, 22000, Algeria.*
[2] *Institute of electronic, University Centre of Saida, Algeria.*

Abstract

Molecular-dynamics simulation has been used to investigate structural, elastic and thermodynamic properties of tin in the temperature range from 200K up to 286.36K. Calculations are carried out using the inter-atomic interactions model like a three-body potential of Tersoff. In the present work, a special interest has been made to the first form of tin (α-Sn), the reason why the temperature is below 286.36K. The calculated results of the lattice constant, the bulk modulus and its derivative, the total energy, and the pair distribution function are correctly described, in excellent agreement with other theoretical works as well as the experimental results. Our study enabled us to predict the thermodynamic properties like the specific heat and lattice thermal expansion.

Key words: MD simulation, Structural, Elastic and thermodynamic properties, Tin.

1. Introduction

Tin is primarily obtained from the mineral cassiterite (SnO_2) and is extracted by roasting cassiterite in a furnace with carbon. Ordinary tin is composed of nine stable isotopes, 18 unstable isotopes are also known. Ordinary tin is silver –white metal, is malleable, and has a highly crystalline structure. Two allotropes of tin occur near room temperature. The first form of tin is called grey tin (α-Sn) and is stable at temperature below 286.2 K. This form crystallizes in the diamond structure [1], in common with the lighter elements in column IV A of the periodic table. At temperature above 286.2 K, grey tin slowly turns into tin's second form, white tin. This second form (β-Sn) is a tetragonal distortion of diamond with two atoms per unit cell [2]. Tin is used to form many useful alloys. Bronze is an alloy of tin and copper. Tin and lead are alloyed to make pewter and solder. An alloy of tin and niobium is used to make superconductive wire. Type metal, fusible metal, bell metal and Babbitt metal are other examples of tin alloys. For a given temperature and a variation of pressure, tin shows a

---

*) For correspondence: sba_soudini@yahoo.fr

transition sequence. These temperature- and pressure- driven phase transformations have caused tin to be of considerable experimental and theoretical interest.

From the theoretical point of view, there are some calculations performed about this material. Among them, calculations using the empirical pseudopotential method (EPM) [3], the full-potential linear muffin-tin orbital method (FP-LMTO) [4], the full-potential linearized augmented plane-wave method (FP-LAPW)], and the tight-binding calculations [5]. There are also some experimental results obtained for this material [6].

It is well known that molecular dynamics simulation have been widely used in many different fields ranging from physical chemistry to solid-state physics to study the microscopic behaviour of temperature-and time-dependent phenomena [7]. A great deal of work has been carried out using classical potentials to describe the interactions between atoms. This approach, with the help of modern computers, allows one to study such relatively slow processes such as phase transition. In the conventional (or *classical*) molecular dynamics approach, a model of inter-atomic interactions must be provided as input before a simulation can be carried out. Such models, or *inter-atomic potentials*, are based on *a priori* knowledge of the physical system studied. Ionic forces can be derived from such model potentials, and atomic trajectories are computed by integrating the Newtonian equations of motion. The classical approach is adequate if one is interested in general to the qualitative properties of materials [8-10]. Quantitative predictions can also be obtained, but this requires a careful choice of the interaction potential. In practice, it is not always possible to find a classical potential that describes the interactions of certain systems in all chemical environments. This transferability problem is particularly severe in the case of materials for which little experimental data is available. This is the case of the α-Sn, which is known to be a semiconductor with a zero band gap (semimetal) and where the knowledge of the dynamic and the thermodynamic properties for this structure phase are essential. This has prompted us to take such calculations for the grey tin.

The aim of the present work is to show that a molecular dynamics simulation method in conjunction with an empirical interaction potentials like the three-body potential of Tersoff, the temperature dependence of the structural and thermodynamic properties of the grey tin are correctly described, in excellent agreement with the theoretical and experimental results.

2. Computational details

The central core of a molecular dynamics simulation is the choice of the interatomic potential, which determines the failure or success of a simulation. There are tens of empirical interaction potentials, which have been used to described elemental semiconductors, semiconductors compounds, metals and more complex systems [11, 12]. Among all these empirical interaction potentials we choose the three-body potential of Tersoff which treats successfully the properties of solids having diamond and zinc-blende structures. As it is a bond-order potential composed of a two-body expansion which depends on the local environment, these bond order models have been shown to describe reasonably well the chemical properties of bonding in covalent materials [13, 14]. Many works have been performed using this models and have showed its effectiveness in the study of the structural, dynamic and thermodynamic properties, for examples the Si [15-17], C [18], and compounds like ZnTe [19], GaN [20], SrO [21], and BP[22].

.
The inter-atomic potential energy between two neighbouring atoms *i* and *j* has the form:

$$V_{ij} = f_c(r_{ij})[Aa_{ij}\exp(-\lambda_1 r_{ij}) - Bb_{ij}\exp(-\lambda_2 r_{ij})] \tag{1}$$

where

$$f_c(r_{ij}) = \begin{cases} 1 & r < R \text{ - } D \\ \dfrac{1}{2} - \dfrac{1}{2}\sin[\dfrac{\pi}{2}\dfrac{(r-R)}{D}] & R\text{-}D < r < R + D \\ 0, & r > R + D \end{cases} \qquad (2)$$

where b_{ij} is the many-body-order parameter describing how the bond-formation energy (the attractive part of V_{ij}) is affected by the local atomic arrangement due to the presence of other neighbouring atoms, (the k-atoms). This many-body function of atomic positions i, j and k has the form [18] :

$$b_{ij} = (1 + \beta^n \xi^n_{ij})^{-1/(2n)} \qquad (3)$$

where

$$\xi_{ij} = \sum_{k \neq i,j} f_c (r_{ik}) g(\theta_{ijk}) exp[\lambda^3{}_3(r_{ij} - r_{ik})^3] \qquad (4)$$

$$g(\theta) = 1 + c^2/d^2 - c^2/ [d^2 + (h - cos\theta)^2] \qquad (5)$$

$$a_{ij} = (1 + \alpha^n n_{ij}{}^n)^{-1/(2n)} \qquad (6)$$

$$n_{ij} = \sum_{k \neq i,j} f_c(r_{ik}) exp[\lambda_3{}^3 (r_{ij} - r_{ik})^3] \qquad (7)$$

where ξ_{ij} is called the effective coordination number and $g(\theta)$ is a function of the angle between atoms and has been fitted to stabilize the tetrahedral structure. Thus, the Tersoff potential has 13 parameters ($A, B, \lambda_1, \lambda_2, \lambda_3, \alpha, \beta, n, c, d, h, R$, and D). These parameters were derived from gray-tin cohesion energy adjustment and are shown in Table 1.

A(eV)	2740.30
B(eV)	537.67
$\lambda_1(A^{0-1})$	2.3548
$\lambda_2(A^{0-1})$	1.6424
$\lambda_3(A^{0-1})$	0.0
α	0.0
β	0.964E-06
n	0.75003
c	101266.29
d	15.590
h	-0.43822
R (A^0)	3.2
D (A^0)	0.15

Table 1: Adjusted Tersoff parameters for Sn in the diamond structure.

During the molecular dynamics simulations, we have taken the number of steps equivalent to 10000, for a system of 216 atoms arranged in a cubic simulation cell by taking into account of the periodic boundary conditions. The simulation is formed of a cube of side L with $3 \times 3 \times 3$ diamond units cells, so that eight atoms per unit cell. To integrate Newtonian equations of motion, the fifth-order predictor–corrector algorithm is used with a time step Δt=1.5 ps and an efficient network cube algorithm for nearest-neighbour book keeping, more details are given elsewhere [23].

3. Results and discussion

3.1 Structural properties

To test the effectiveness of the interaction potential and then our adjusted parameters, we have computed the structural properties of tin for different temperatures. Simulation is started from an initial structure, in which the two atoms are placed on a diamond lattice. After the system passed to the equilibrium state, we calculated the pair distribution function $g(r)$ at various temperatures. The pair distribution function is the probability of finding another atom at a distance r from a specified atom. Among the several static structural information that can be obtained from the pair distribution function as bond length, atomic bond angle distributions, crystalline symmetry, and coordination numbers, it's variation with the temperature and pressure gives information about structural phase transitions. Moreover, the variation with the temperature provides directly the thermal expansion coefficient while the width of the g(r) gives the atomic oscillation amplitude, which permits to calculate the dynamical Debye-Waller factor. We have illustrated as in fig.1, the pair distribution function *g(r)* for Sn. We notice large peak at a small distances and the bond length (Sn-Sn bond distance) corresponds to the maximum peak position. From the full width of the pair distribution function we can obtain the atomic oscillation amplitude for Sn-Sn atoms. At larger distances, the peaks decrease in amplitude indicating a long-range order characteristic of the solid state. From the first peak, we have deduced the coordination number N according to the equation [19]:

$$N = 4\rho_0 \, \pi \int_0^R r^2 g(r) \, dr \tag{8}$$

where ρ_0 is the number density of atoms and R, denotes the position of the first minima in *g(r)*.

Sn		
1 st peak	Distances (A°)	2.803
	Number of pair:	3.944 (4)
2nd peak	Distances (A°)	4.555
	Number of pair	11.898 (12)
3rd peak	Distances (A°)	5.373
	Number of pair:	11.91 (12)
4th peak	Distances (A°)	6.464
	Number of pair:	5.969 (6)

Table 2: The values of peaks distances and coordinate numbers of pairs for Sn at T= 253K.

In table 2, the values of the number N as well as the peak positions are given for T=253K. For this considered temperature, we notice that from the first peak the coordination number is four. When the distance increases the coordination number increases for the second and the third peaks. The coordination number becomes six-fold for the fourth peak.

Let us now consider the effect of the temperature on the pair distribution function (figure1 (a,b,c)) where we notice an important resemblance with a small evolution peaks amplitudes of $g(r)$ versus the temperature. The relative variation of amplitude for the first peak is 4.9% when the temperature changes from 253 to 286K. The increase of the temperature affects then the peaks position which implies the lattice expansion. The calculated values of N from Eq. (8) for the three temperatures 253K, 273K and 286K are approximately equal to four showing that the diamond structure of tin is preserved.

Sn	a (A°)	B_0(Mbar)	B_0'	E_{coh} (eV)
Present work	6.490 (12.268 Bohr)	0.488	4.91	-3.109
LAPW	6.469 (12.23 Bohr) [a]	0.45. [a]		
TB	6,474 (12.24 Bohr) [a]	0.45.[a]		
Other	6,546 (12,376 Bohr) [b]	0..51 [b]		-3.12[d]
Experiment	6.487 (12.263 Bohr) [c]	0.53. [b]		-3.12[e]

	Present work	TB[a]	Experiment[a]
B_0 (Mbar)	0.488	0. 436±0.01	0.4653±0.005
C_{11}- C_{12} (Mbar)	0..320	0.376±0.007	0. 3024±0.0 11
C_{11} (Mbar)	0.701	0.677±0.015	0.6667± 0.007
C_{12} (Mbar)	0.381	0.301±0.012	0.3645 ±0.004
C_{44} (Mbar)	0.368	0.38±0.01	0.302±0.002

Table 3: Equilibrium lattice parameter and elastic constants of Sn in the diamond structure at 286K. [a] Reference [5], [b] Reference [4], [c] Reference [1], [d] Reference [26], [e] Reference [27]

To simulate the temperature effect on the energy, we have computed the total energy per molecule as a function of volume for tin. To determine the static properties of the phase under study (equilibrium lattice constant *a,* bulk modulus B_0 and its pressure derivative B_0') we use the Murnaghan equation of state [24] to fit our calculated E-V data. The results are given in Table 3 for T=286K, and we note that our lattice constant and the cohesive energy E_{coh} are in good agreement with experimental results. In figure 2, we have displayed the E-V diagram for three temperatures where the equilibrium volumes correspond to the minimum energy and then the stability of this structure for the considered temperature.
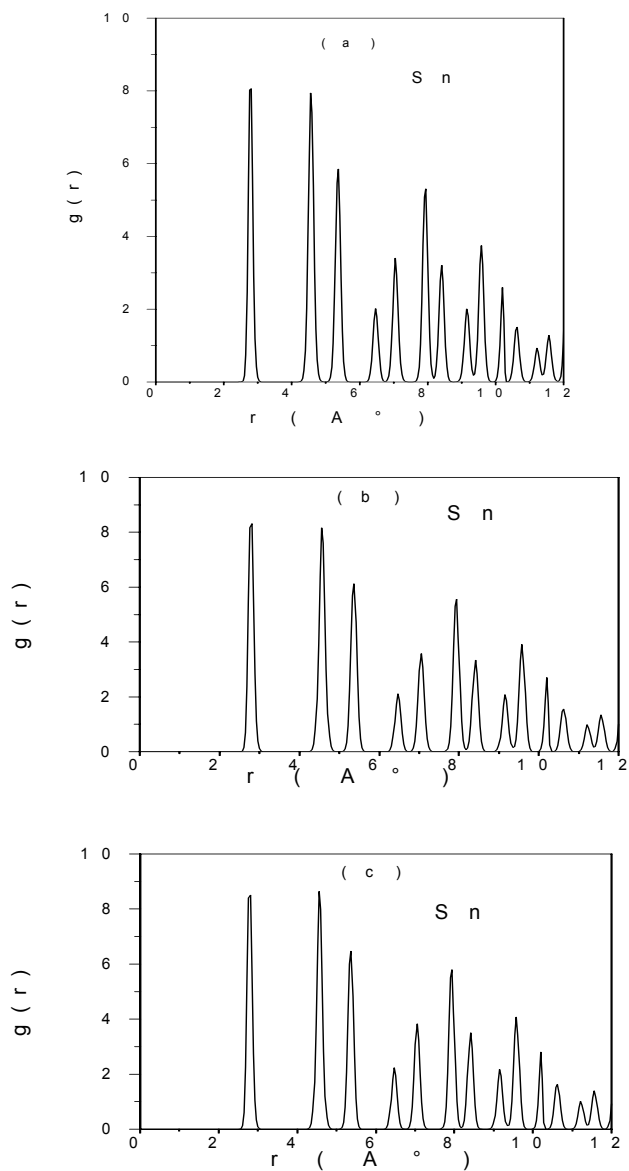
Fig. 1: The pair distribution function of Sn in the diamond structure at a) T=253K, b) T=273K and c) T=286K(c).
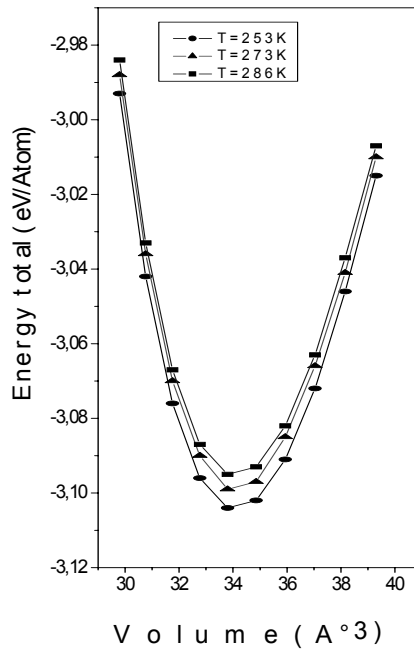
Fig.2: The total energy versus the volume, at 253K, 273K and 286K.

It is well-known that the elastic properties define the properties of material that undergoes stress, deforms, and then recovers and returns to its original shape after stress ceases. Hence to study the stability of this material in the diamond structure, we have calculated the elastic constants (C_{11}, C_{12} and C_{44}) using the standard method of Mehl [25].

The results of the elastic constants are listed in Table 3, where we found an agreement between our results and that of experiment. But the value of C_{44} is underestimated compared to the experiment. Note that in the diamond structure of tin which has a cubic lattice, there are only three independent elastic constants C_{11}, C_{12} and C_{44} related to the bulk modulus. The calculation of the bulk modulus and C_{11}-C_{12} requires no relaxation of the atomic positions, but the calculation of C_{44} requires the relaxation of one internal coordinate.
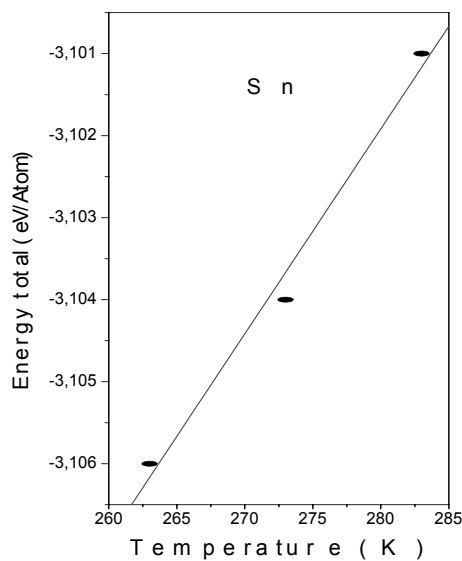

Fig. 3: Total energy versus temperature of Sn for the diamond Structure.

It is clear from the curve of the cohesive energy versus temperature (figure 3) that the diamond structure of tin remains unchanged. This is a consistent with the fact that at

47

temperature below 286.2 K the first form is the α-Sn. From these results we have deduced the heat capacity of the system at constant volume given by:

$$C_v = \left(\frac{\partial E}{\partial T}\right)_{/V} \tag{9}$$

A linear equation is fit to the calculated energy-temperature results at each volume to derive C_V where we find $Cv=24.08\ J\ K^{-1}.mole^{-1}$. This value is in agreement with that of the literature [25].
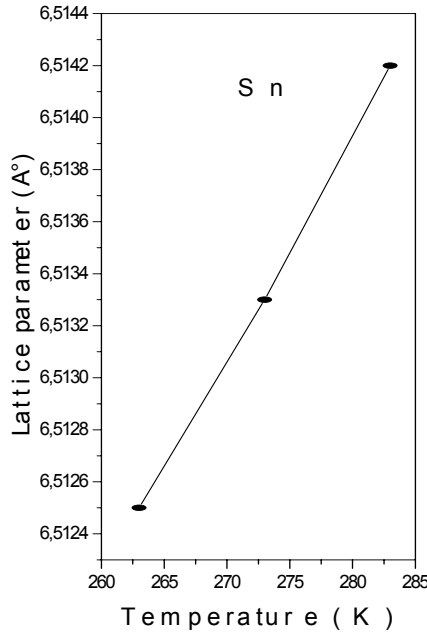

Fig. 4: Lattice parameter of Sn versus temperature for diamond structure.

To analyse the effect of the temperature on the lattice, we illustrate in figure 4 the variation of the lattice constant with temperature. We notice that the lattice parameter increases as the temperature increases. This behaviour leads us to state that the thermal expansion coefficient follows the same trend. This coefficient is computed directly from the following relation [21]:

$$\alpha = \frac{1}{a}\left(\frac{\partial a}{\partial T}\right)_{/p} \tag{10}$$

where a is the lattice constant. To check the rigidity of the crystal, we have computed the bulk modulus versus the temperature where the polynomial fit of our data is given by the equation:

$$B_0 = -1.90476\ 10^{-4}\ T^2 + 0.1039T - 13.67 \tag{11}$$

This equation explains that when the temperature increases the bulk modulus decreases.
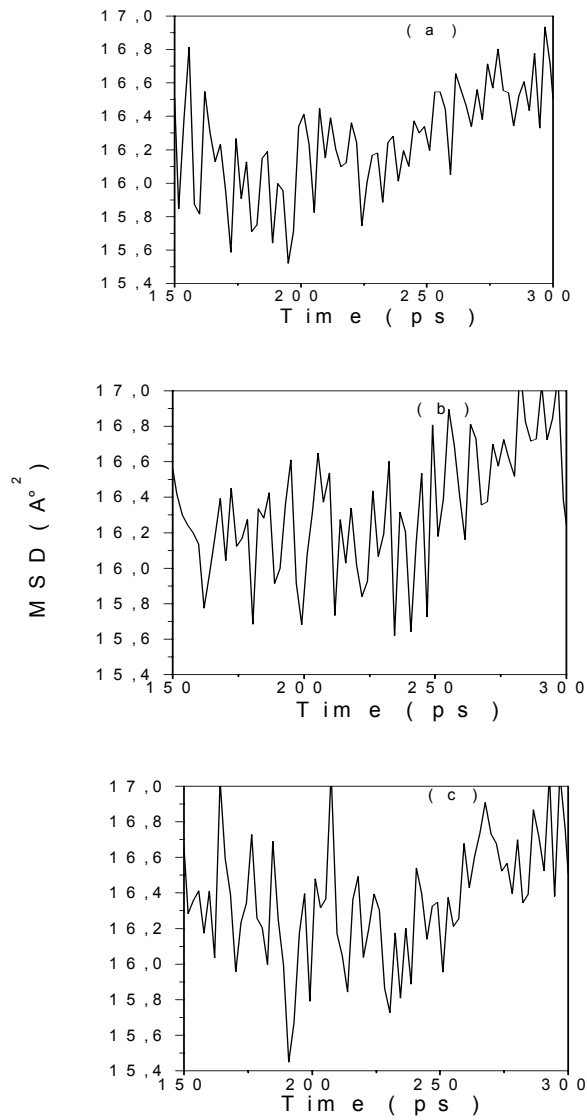
Fig. 5: Time dependence of the mean-square displacement in tin at a) 253K, b) 273K and c) 286K.
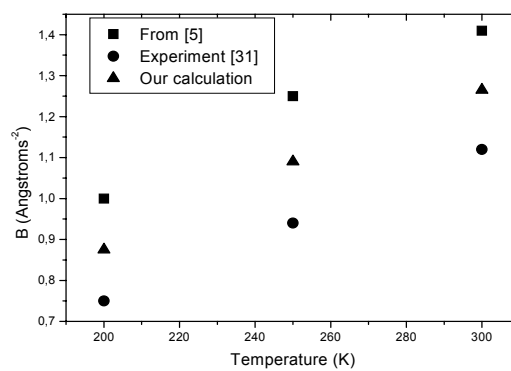

Fig. 6: The Debye-Waller factor versus the temperature (solid squares [5], solid triangles present work and solid circles from experiment [31]).

This is a consistent with the fact that the increase of temperature causes an expansion of the lattice and then the tetragonal distortion of diamond, which becomes less rigid leading us to state that for the temperature above 286 K we obtain new phase for tin (β-Sn).

In order to correctly obtain the information about the Debye temperature of solid Sn, when quantum effects can be neglected, we have used the empirical relation taken by [28], our calculated Debye temperature is $\Theta_D=233K$. This value is close to the experimental result (200K) [29] by 16%.

3.2 Dynamical properties

Finally, we have used this simulation to compute the mean square deviation (*MSD)* of the atoms, defined as [30]:

$$MSD=\left\langle\left|r(t)\right|^2\right\rangle=\frac{1}{N}\sum_{i=1}^{N}\left\langle\left|\vec{r}_i(t+t_0)-\vec{r}_i(t_0)\right|^2\right\rangle \tag{12}$$

Where $\vec{r}_i(t_0)$ and $\vec{r}_i(t+t_0)$ are the positions of *ith* atom at the start and end of the time interval *t*. The *MSD* for a given time *t* is then calculated by averaging over time origins *(t₀)*. The calculated *MSD* as a function of the time is shown in fig. 5(a,b,c) at 253K, 273K and T=286K**.** From figure 5, we notice that the MSD presents various fuctuations when time increases and the shape of the peaks is affected by the change of temperature**.** This result thus reflects the thermodynamic behavior of tin.

The *MSD* is connected to the Debye-Waller factor *B* by the relation

$$B = 8\pi^2\left\langle u_x^2\right\rangle = \frac{8}{3}\pi^2\left\langle\left|r\right|^2\right\rangle \tag{13}$$

where $\left\langle u_x^2\right\rangle$ is the thermal average of the mean square displacement in the *x* direction. By symmetry, this is just one third of the total mean square displacement of the atoms, $\left\langle\left|r\right|^2\right\rangle$

We notice from figure 6 that this factor increases with temperature. This result is in agreement with the experiment [31].

4. Conclusion

In this paper, we have reported successful calculations of structural, elastic and thermodynamic properties of tin using molecular-dynamics simulation. As an inter-atomic interactions potential that describes the interactions of the studied system in all chemical environments, we have used a three-body potential of Tersoff. The results of our calculations show an agreement with the experimental results as well as other theoretical works. We have also interested to the effect of the temperature on the structural and thermodynamic properties, especially between the Debye temperature (200 K) and that of the diamond phase stability. Finally, we state that the molecular-dynamics simulation with the three-body potential of Tersoff is an extremely powerful technique, suggesting that its extension to more complicated structures like the ternary or quaternary semiconductors alloys and metastable alloys will produce satisfactory results as well.

References

[1] P. Villars, and L. D. Calvert (editors), 1991, Pearson's Handbook of Crystallographic Data for Intermetallic Phasesn second edition (Materials Park, Ohio American Society for Metals)

[2] G. Simmons, and H. Wang, 1971, Single Crystal Elastic constants and Calculated aggregate Properties: A Handbook, second edition (Cambridge, Massachusette, MIT Press).

[3] B.Soudini**,** H.Aourag and B.Khelifa, Phys. Stat. Sol. (b) **167** (1991) 139

[4] N. E. Christensen, and M. Methfessel, Phys. Rev. B **48** (1993) 5796

[5] B. Akdim, D.A. Papaconstantopoulos, and M. J. Mehl, Phil. Mag. B **82** (2002)47

[6] L. J. Slutsky and C. W. Garland, Phys. Rev. **113** (1959), 167 and references therein.

[7] Simulation of liquids and solids, eds. G. Ciccotti, D. Frenkel and I. R. McDonald (North-Holland, Amsterdam, 1986)

[8] C. Massobrio, V. Pontikis and G. Martin, Phys. Rev. B **41** (1990)10486

[9] Y. Limoge, A. Rahman, H. Hsieh and S. Yip, J. Non-Cryst. Solids **99** (1988) 75

[10] R. Car and M. Parrinello, Phys. Rev. Lett. **55** (1985)2471

[11] F. H. Stillinger and T. A. Webern Phys. Rev. B **31** (1985) 5262

[12] S. Erkoç, Phys. Reports **278** (1997) 79 (in this paper several empirical interaction potentials are discussed).

[13] A. P. Horsfield, A. M. Bratkovsky, M. Fearn, D. G. Pettifor, M. Aoki, Phys. Rev. B **53** (1996) 12694

[14] M. Z. Bazant, E. Kaxiras, and J. F. Justo, Phys. Rev. B **56** (1997) 8542

[15] J. Tersoff, Phys. Rev.B **37** (1988)   6991

[16] J. Tersoff, Phys. Rev.B **39** (1988) 9902

[17] J. Tersoff, Phys. Rev.Lett. **61** (1988) 2879

[18] J. Tersoff, Phys. Rev.B **39** (1989) 5566

[19] M. B. Kanoun and al , Solid State Sciences **5** (2003) 1211

[20] F. Benkabou and al.: phys. stat. sol. (b) **209** (1998) 223

[21] F. Z. Aoumeur-Benkabou, B.Belgoumène: computer coupling of phase Diagrams and thermochemistry **28** (2004) 65

[22] F. El-Mellouhi, W.Sekkal, A.Zaoui, Physica A **311** (2002) 130

[23] M. A. Shahzamanian, J. Phy. Condens. Matter **1** (1989) 1965

[24] F. D. Murnaghan, proc. Natl. Acad. Sci. USA **30** (1944) 5390

[25] M. J. Mehl, Phys. Rev. B **47** (1993) 2493

[26] A. Chen, A. Sher. Semiconductor alloys: Physics and material engineering (Plenum Press, N.Y., 1995)

[27] C. Kittel. Introduction to the physics of the solid state. 3rd. edition, p96 (1981)

[28] W. Sekkal, H.Aourag, M.Certier, Comput. Mater. Sci. **9** (1998) 295

[29] Jean-Pierre SARMANT, Dictionary of physics, Hatchet Edition, p15 (1981)

[30] B. B. Karki, D. Bhattarai, and L. Stixrude Phys. Rev. B. **73** (2006) 174208

[31] L. Peng, G. Ren, S. Dudarev, M. Whelan, Acta crystallogr. A. **52** (1996) 456